Positron scattering from formic acid

Antonio Zecca and Luca Chiari
Department of Physics, University of Trento, I-38050 Povo (Trento), Italy

A. Sarkar
Department of Physics, Bangabasi Morning College, 19 R. C. Sarani, Kolkata 700 009, India

Marco A. P. Lima
Instituto de Física Gleb Wataghin, Universidade Estadual de Campinas, Caixa Postal 6165, 13083-970, Campinas, SP, Brazil

Márcio H. F. Bettega
Departamento de Física, Universidade Federal do Paraná, Caixa Postal 19044, 81531-990, Curitiba, Paraná, Brazil

Kate L. Nixon and Michael J. Brunger
ARC Centre for Antimatter-Matter Studies, School of Chemistry, Physics and Earth Sciences, Flinders University, GPO Box 2100, Adelaide, SA 5001, Australia

(Received 27 July 2008; published 20 October 2008)

We report on measurements of total cross sections for positron scattering from the fundamental molecule formic acid (HCOOH). In this case, the energy range of our experimental work is 0.3–50.2 eV. Our interpretation of these data was somewhat complicated by the fact that at room temperature, formic acid vapor consists of about 95% monomer and 5% dimer forms, so that the present cross sections represent an average for that ensemble. To assist us in interpreting the data, rigorous Schwinger multichannel level calculations for positron elastic scattering from the formic acid monomer were also undertaken. These calculations, incorporating an accurate model for the target polarization, are found to be in good qualitative agreement with our measured data, particularly when allowance is made for the target beam mixture (monomer versus dimer) in the experiment.

DOI: 10.1103/PhysRevA.78.042707 PACS number(s): 34.80.Uv, 34.80.Bm, 34.80.Gs, 25.30.Hm

I. INTRODUCTION

The seminal paper of Boudaiffa *et al.* [1] questioned the belief that ballistic impacts were responsible for the majority of cell and tissue damage when ionizing radiation, such as positrons used in positron emission tomography (PET), enters the body. Indeed it is now accepted that when this high-energy ionizing radiation enters the body, it liberates many low-energy secondary electrons that can in turn attach to the various components of DNA (i.e., the bases, sugars, and water). Through the process of dissociative attachment, this leads to single or double DNA strand breaks, or the formation of free radicals, which through chemical reactions with DNA can also lead to strand breaking [1]. It is therefore not surprising that significant recent work has been devoted to electron scattering from biomolecules in general and formic acid (HCOOH) in particular. These formic acid studies have been both experimentally [2–6] and theoretically based [7–9] and have yielded much important information on its dissociation dynamics and absolute cross-section measurements. Note that formic acid, the simplest organic acid, is thought to play a major role in the formation of the larger biomolecules such as glycine and acetic acid. Furthermore, the formate group (–COOH) is a key component of more complex biomolecules including some of the amino acids.

We stress here that the mechanisms leading to biological damage are quantitatively different for positrons and electrons. In fact, while positron and electron total cross sections merge at energies above a few keV, they are quite different at energies below a few tens of eV [10]. Qualitatively, the presence of the positronium formation channel makes an even larger difference for positron scattering, as in diagnostic and real treatment situations the final fate of the positrons is to be annihilated inside the organic tissue, which adds the ionizing effects of the annihilation gamma rays.

Our knowledge with respect to positron scattering from formic acid is, however, rather poor. Hence we have undertaken this joint theoretical and experimental study. Formic acid represents an excellent system for benchmarking positron-molecule interactions. It is highly polar (1.41 D) and has a large dipole polarizability (~22.5 a.u.), yet it is a small enough molecule to render quite sophisticated calculations, which need to account for these and other physical effects, tractable. For example, the overall potential experienced by the positron during the collision comes from adding the negative polarization potential to the positive static one. If both potentials are equivalently strong, this cancellation becomes very sensitive to small errors in their construction. Hence accurate experimental data, such as we report here, can be invaluable in assisting the development of theory.

In this paper, we continue our experimental investigations into positron scattering from important biomolecules by considering formic acid, having previously reported results on water [11], tetrahydrofuran [10], and 3-hydroxytetrahydrofuran [12]. In the next section, we briefly describe the experimental details of our measurements, while in Sec. III, the current theory and our relevant computational details are provided. Thereafter, in Sec. IV, our theoretical and ex-

perimental results are presented and discussed. Finally, in Sec. V, some conclusions from the present study are drawn.

II. EXPERIMENTAL DETAILS AND ANALYSIS TECHNIQUES

The current positron spectrometer was developed by Zecca and co-workers and has already been previously described in some detail [13]. As a consequence, we do not repeat that detail here, except to note that our source of positrons is a radioactive ^{22}Na isotope that is employed in conjunction with a tungsten moderator. We further note that it is standard practice in our laboratory, as a check to the validity of our measurement techniques and procedures, to perform preliminary measurements from molecular nitrogen (N_2). Molecular nitrogen was chosen because of the availability of a nice set of data from Hoffman *et al.* [14], against which we could benchmark our results. In general, excellent agreement, over the common energy range and to within the respective cited errors, was found between the present e^+-N_2 total cross sections and those from Hoffman *et al.* [14].

The basis of the present measurements is the Beer-Lambert law, as given by

$$I_1 = I_0 \exp\left(\frac{-(P_1 - P_0)L\sigma}{kT}\right), \tag{1}$$

where I_1 is the positron beam count rate at P_1, the pressure measured with HCOOH routed to the scattering cell, k is Boltzmann's constant, T is the temperature of the gas (in K), σ is the total cross section, I_0 is the positron beam count rate at P_0, the pressure with the HCOOH diverted to the vacuum chamber, and L is the length of the scattering region.

For a correct application of Eq. (1), several important precautions need to be taken and care must be exercised during the measurements. Those considerations include minimizing double-scattering events and ensuring that the total cross sections (TCSs) are pressure-independent. These were achieved by keeping the ratio I_1/I_0 to values larger than 0.7 and by checking the linearity of the plots of $\ln(I_1/I_0)$ versus pressure at selected energies. In addition, high-purity formic acid was used throughout this study, with several freeze-pump-thaw cycles employed to ensure it was appropriately degassed. Nonetheless, room-temperature formic acid does present some challenges to the experimentalist. Foremost among them is that the formic acid sample will consist of both its dimer and monomer forms, with the degree of dimerization depending on the pressure and temperature of the HCOOH sample [15]. Following the prescription of Taylor and Bruton [16], the % dimer target composition as a function of sample pressure, at room temperature (~24 °C), can be calculated with the result of this process being given in Fig. 1. Figure 1 indicates that for the typical sample pressures of this study, a beam composition of ~5% dimer and 95% monomer is expected, so that the present TCSs represent an average for that ensemble. The formic acid monomer also has two stable planar forms, the *cis* and *trans* isomers. The energy difference between the two isomers in the gas phase is 1365 cm^{-1} (0.169 eV) [4], so that a Boltzmann calculation of the population ratio at room temperature indicates a clear predominance of the *trans* form (~1000 times more abundant) in our sample.

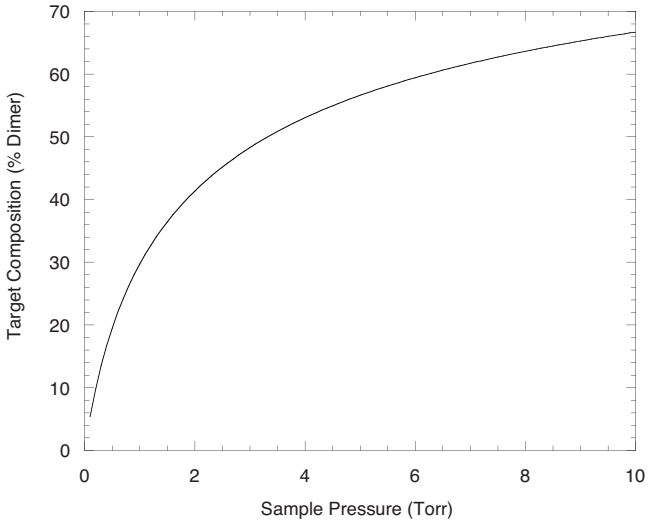

FIG. 1. % dimer target composition as a function of formic acid sample pressure (Torr) at room temperature (24 °C).

The geometrical length of the scattering region is 22.1 ± 0.1 mm, with apertures of 1.5 mm diameter at both the entrance and exit of the scattering chamber [13]. End effects [10] were also considered in the current investigation. It has been demonstrated [17], however, that the effects due to the entrance and exit apertures cancel if the two apertures have equal diameters, so that in our geometry their contribution to the uncertainty in the value of L is possibly less than 0.2%. In our application of Eq. (1), the value of L used has been corrected to account for the path increase caused by the gyration of the positrons in the focusing axial magnetic field (~8–10 G) present in the scattering region (typically this correction was ~5% here). The gyration of the projectile particles can also potentially increase the angular resolution error with respect to the no-field case [18]. However, absolute differential cross sections for e^+-HCOOH scattering are not currently known, so that a correction for this effect cannot be made. We note that if such differential cross sections were available, then the true TCS would be somewhat larger than the values published in Table I and Figs. 2 and 3 with no correction. We further note that, at worst, we estimate the angular resolution of the present apparatus to be ~0.017 rad.

It is essential in these types of studies that the energy scale is calibrated accurately. The zero for the energy scale, in the absence of the target gas, was determined here with a retarding potential analysis of the beam [19]. This measurement suggests a probable error of ±0.2 eV in our energy scale, and an energy width of the positron beam of ~0.3 eV (full width at half-maximum). It is also crucial to measure accurately the scattering cell pressure, which was achieved with a MKS Baratron capacitance manometer (Model 628B, 1 Torr full scale) operated at 100 °C. Since the scattering chamber was at room temperature (24 ± 2 °C), a thermal transpiration correction has been applied to the pressure readings. This correction has been calculated according to the model of Takaishi and Sensui [20], and is less than 10% over the entire energy range. The value of the formic acid

TABLE I. The present experimental total cross sections (10^{-16} cm^2) for positron scattering from formic acid. The errors given represent one standard deviation on the measured cross section at a given energy.

Positron energy (eV)	Cross section (10^{-20} m^2)		Positron energy (eV)	Cross section (10^{-20} m^2)	
	Value	Error		Value	Error
0.3	161.0	10.6	6.95	17.1	0.4
0.35	154.9	13.8	7.2	16.2	0.5
0.4	113.2	7.6	7.45	15.7	0.6
0.5	109.1	11.9	7.7	16.8	0.5
0.6	82.2	5.3	7.95	16.4	0.1
0.7	70.8	4.2	8.2	16.3	0.4
0.8	62.1	3.6	8.45	16.3	0.1
0.9	57.3	1.3	8.7	16.2	0.6
1.0	49.5	1.9	9.2	16.3	0.4
1.1	48.1	3.2	9.7	16.6	0.2
1.2	46.5	1.8	10.2	16.1	0.2
1.3	44.9	1.1	11.2	16.1	0.1
1.6	36.3	1.9	12.2	15.9	0.2
1.8	31.6	1.2	13.2	15.6	0.6
2.2	28.9	0.8	14.2	15.1	0.1
2.7	25.7	1.0	15.2	15.4	0.1
3.2	22.2	0.5	16.7	14.8	0.2
3.7	21.5	1.4	20.2	14.8	0.2
4.2	19.1	1.0	22.2	14.4	0.2
4.45	18.7	0.6	24.7	14.8	0.1
4.7	18.3	0.7	28.2	14.6	0.0
5.2	17.9	0.4	31.7	14.3	0.4
5.45	17.8	0.1	37.7	14.0	0.3
5.7	17.1	0.3	40.2	13.7	0.1
5.95	17.0	0.3	43.2	13.2	0.2
6.2	16.8	0.6	45.2	12.9	0.4
6.45	16.5	0.1	50.2	12.5	0.3
6.7	16.6	0.4			

molecular diameter used in this correction was taken from Vizcaino *et al.* [4], and was 3.8 Å.

The data collection and analysis codes were driven by software developed at the University of Trento, for application on a personal computer. Measurement time at each discrete energy was about 1 h, with each point being the average of typically 100 single determinations. Note that the standard deviation of that average was also calculated from these data, with these errors being given in Table I along with the present TCSs. The positron beam obtained with our apparatus [13] is typically very stable over times ~1 month, and all the TCS results reported were taken under stable positron beam conditions. The absolute errors on our measurements (not given in Table I) were evaluated as the root of the quadratic sum of the contributing errors. A detailed discussion of these contributions is given elsewhere [21], and in the references contained within that paper. Note that the uncertainty in the thermal transpiration and *B*-field corrections is ~0.3%, with the uncertainty in these corrections being treated as additional sources of systematic error. Clearly they do not contribute significantly to the overall systematic uncertainty in our measurements. Indeed we further note that the absolute TCS errors on our formic acid data were typically in the range 5–9 %, with the larger errors only occurring at the lowest energies.

III. THEORY AND COMPUTATIONAL DETAILS

To compute the elastic cross sections, we employed the Schwinger multichannel method (SMC) developed for studying positron-molecule collisions. This method has been described in detail in several publications [22–24] and so here we will only discuss those points that are relevant to the present calculations.

The working expression to the scattering amplitude is

$$f(\vec{k}_f,\vec{k}_i) = -\frac{1}{2\pi}\sum_{m,n}\langle S_{\vec{k}_f}|V|\chi_m\rangle(d^{-1})_{mn}\langle\chi_n|V|S_{\vec{k}_i}\rangle, \qquad (2)$$

where

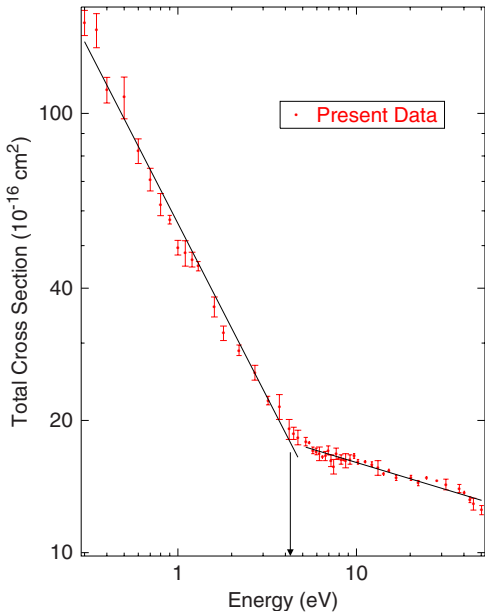

FIG. 2. (Color online) The present experimental total cross sections (10^{-16} cm^2) for positron scattering from formic acid. The lines are the least-squares fits to the two subsets of points on the right and left, where the division is chosen to give the largest ratio of the slope on the left to the slope on the right, subject to the condition that each subset contains at least 10 points. The lines intersect at 4.3 eV.

$$d_{mn} = \langle \chi_m | A^{(+)} | \chi_n \rangle \tag{3}$$

and

$$A^{(+)} = Q\hat{H}Q + PVP - VG_P^{(+)}V. \tag{4}$$

In the above equations, $|S_{\vec{k}_{i,f}}\rangle$ is a solution of the unperturbed Hamiltonian H_0 (the kinetic energy of the incoming positron plus the target Hamiltonian) and is a product of a target state and a plane wave, V is the interaction potential between the incident positron and the electrons and nuclei of the target, $|\chi_m\rangle$ is a set of $(N+1)$-particle configuration state functions (CSFs) used in the expansion of the trial scattering wave function, $\hat{H}=E-H$ is the total energy of the collision minus the full Hamiltonian of the system, with $H=H_0+V$, P is a projection operator onto the open-channel space defined by the target eigenfunctions, and $G_P^{(+)}$ is the free-particle Green's function projected onto the P space. Finally, $Q(=\mathbb{1}-P)$ is the projector onto the closed electronic channels of the target.

The direct space is composed by CSFs of the form:

$$|\chi_i\rangle = |\Phi_1\rangle \otimes |\varphi_i\rangle, \tag{5}$$

where $|\Phi_1\rangle$ represents the ground state of the molecule obtained at the Hartree-Fock level and $|\varphi_i\rangle$ is a one-particle function that represents the incoming positron. The set composed by these one-particle functions is used as the scattering orbitals. Note that the calculations performed in the static approximation consider only CSFs from the direct space and the set of scattering orbitals $|\varphi_i\rangle$ can therefore be represented by the virtual orbitals (VOs) obtained in a Hartree-Fock calculation.

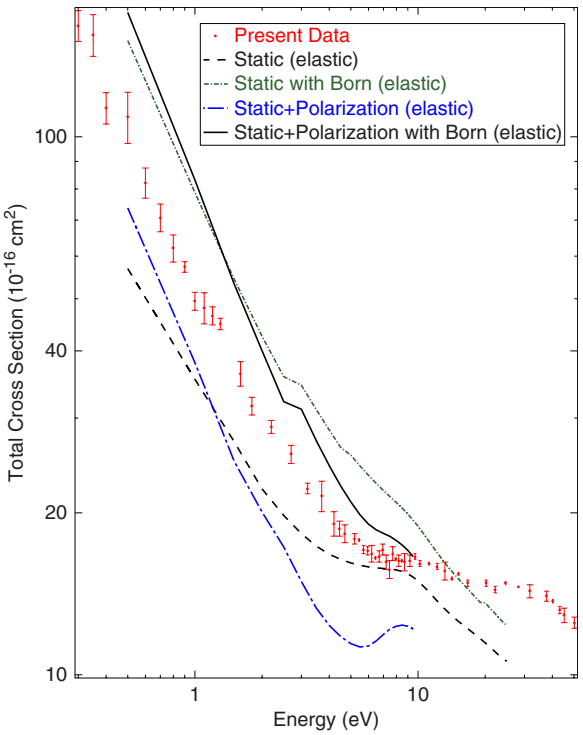

FIG. 3. (Color online) The present experimental (●) total cross sections and theoretical elastic cross sections (both in 10^{-16} cm^2) for positron scattering from formic acid. The static level (---), static plus Born dipole correction (–·–), static plus polarization (·—·), and static plus polarization plus Born dipole correction (——) results are shown.

Polarization effects are incorporated in the calculations by enlarging the direct space by using CSFs of the closed space. These CSFs are constructed as

$$|\chi_{ij}\rangle = |\Phi_i\rangle \otimes |\varphi_j\rangle, \tag{6}$$

where $|\chi_{ij}\rangle$ is obtained by making single (virtual) excitations of the target from the ground state used as a reference state. These excitations are virtual in the sense that they do not allow any energy transfer (in the asymptotic region) between the positron and the target. Furthermore, the target initial and final states correspond to the molecular ground state, and therefore the collision is purely elastic (i.e., all inelastic channels are closed.) The $|\varphi_j\rangle$ is again here a one-particle function. The choice of the orbitals to represent the particle (unoccupied) orbitals and scattering orbitals will be discussed below.

Our present calculations were performed in the static and in the static plus polarization approximations in the C_s symmetry group. We used the ground-state equilibrium geometry of the *trans*-isomer, as given in Ref. [25]. Further, we employed the 6-311++$(3d,1p)$ basis set in both the bound state and the scattering calculations.

As noted above, to take polarization effects into account, we considered single excitations from the hole (occupied) orbitals to a set of particle (unoccupied) orbitals. In the present calculations, we considered all the occupied orbitals as hole orbitals. The choice of orbital to represent the particle

and scattering orbitals, in order to construct a closed space that is not too large but is able to describe properly the polarization effects, is crucial. In this respect, we chose to employ the modified virtual orbitals (MVOs) [26]. These MVOs were generated by diagonalizing a +4 cationic Fock operator and are made orthogonal to the occupied orbitals. We can then use a criterion based on the energies of the MVOs. In the present calculations, we considered excitations to MVOs with energies less than −10 hartree. Note that the same set of MVOs was also used as the scattering orbitals. With this procedure, we obtained 5232 CSFs for the A' symmetry and 4394 CSFs for the A'' symmetry. The use of MVOs to describe both the particle and scattering orbitals has been shown to be an efficient way to describe polarization effects in electron-molecule collisions [27–29], and we expect it also to be applicable here.

In order to analyze the role of numerical stability in the present calculations, we followed a check procedure developed by Chaudhuri and co-workers [30]. This procedure begins with the diagonalization of the matrix elements of the $\tilde{V}$ operator,

$$\tilde{V} \equiv Q\bar{H}Q + PVP, \tag{7}$$

where V and P have already been defined and $\bar{H}=\hat{H}$ is calculated at a fixed energy, following Ref. [30]. A next step consists in the identification and elimination of the configurations weakly coupled by this average potential. That is, the eigenvectors associated with the eigenvalues near zero in the equation $\tilde{V}|\tilde{\chi}_m\rangle = v_m|\tilde{\chi}_m\rangle$ are eliminated. The $\tilde{\chi}_m$'s are then used as the new $(N+1)$-particle basis functions.

As noted earlier, formic acid has a permanent dipole moment. Our calculated value is 1.71 D, which agrees well with the experimental value of 1.41 D [25]. To take the long-range dipole interaction into account in our calculations, we used the standard Born closure on the scattering amplitude. The details of the Born closure are as follows [28]. The SMC amplitude is computed in the body reference frame embedded in the target molecule (this frame allows use of the molecular symmetry). The scattering amplitude of the point-dipole potential, evaluated in the first Born approximation (FBA), is also computed in the body frame. Note that we employed for the point dipole the same orientation and magnitude as the molecular dipole used in the SMC calculations. These two amplitudes are expanded in partial waves up to ℓ_{SMC} and then subtracted from each other. The resulting amplitude is rotated to the laboratory reference frame, where the z axis coincides with the incident positron direction ($\mathbf{k}_i = k_i\hat{\mathbf{z}}$). In the laboratory frame, a closed form to the point dipole can be obtained in the FBA. This closed form is added to the resulting amplitude obtained in the body frame, with the outcome of this procedure being equivalent to replacing the low partial waves of the point-dipole FBA amplitude by the low partial waves obtained by the SMC amplitude. A small inelasticity is considered here (i.e., k_i is slightly different from k_f), in order to avoid divergence in the very forward angle direction. The choice of ℓ_{SMC} is a little complicated, but is defined by the ℓ which provides differential cross sections, obtained using the Born closure and the SMC method, that match for scattering angles above ~30°. The idea behind this choice is that the low partial waves are well described by the SMC method and the high partial waves are described by the FBA of the dipole potential. In the present calculations, we chose $\ell_{\mathrm{SMC}}=1$ from 0.5 to 2.5 eV, $\ell_{\mathrm{SMC}}=4$ from 3 to 4.5 eV, $\ell_{\mathrm{SMC}}=5$ from 5 to 19 eV, $\ell_{\mathrm{SMC}}=6$ from 20 to 30 eV, and $\ell_{\mathrm{SMC}}=7$ at 40 and 50 eV.

IV. RESULTS AND DISCUSSION

In Table I and Fig. 2, we show the present experimental total cross section results for positron scattering from formic acid. In Fig. 2, we also attempt to determine the positronium formation threshold for formic acid from our TCS results. To this end lines of best fit, which seek to highlight at about what energy the monotonic decrease in the TCS with energy changes slope, are plotted. In this case, Fig. 2 indicates that the slope is seen to change at $\sim 4.3 \pm 0.3$ eV. As the first ionization potential (V_i) for the formic acid monomer and dimer is 11.4 ± 0.2 eV [25], and as the general rule [31] is that the positronium threshold energy (E_{P_s}) can be obtained from

$$E_{P_S} = V_i - 6.8 \text{ eV}, \tag{8}$$

we find that $E_{P_s} = 4.6 \pm 0.2$ eV for formic acid. This value for the positronium threshold is consistent with that determined from Fig. 2, so that the energy where the TCS changes slope is indicative for the positronium channel becoming open. It is also manifest from Fig. 2 that the opening of this channel has a significant effect on the magnitude of the TCS above that threshold energy.

The present experimental and theoretical results are presented in Fig. 3. Our theoretical results with polarization effects are shown only for energies up to 10 eV. For energies above 10 eV, the results with polarization display several pseudoresonances that may be due to the closed channels that should be open at those energies. The calculated (elastic) integral cross section qualitatively follows the measured (total) cross-section data for all energies. The calculated cross sections obtained in the static and static plus polarization approximations without considering the Born closure lie below the experimental data. With the inclusion of the dipole interaction the calculated cross section becomes larger than the experimental cross section at all energies.

As the elastic SMC calculation, which includes the static, polarization, and dipole interactions, is the most physical, we now concentrate our discussion on a quantitative comparison between it and our experimental TCS results. We begin by noting that of course it is unphysical for an elastic integral cross section to be greater in magnitude than the corresponding total cross section (see Fig. 3). We believe that there are five possible causes for this observation here, all of which might be making a contribution. First, as noted earlier in Sec. II, the present TCSs are not corrected for forward angle scattering effects. If such a correction were possible at this time, it would have the effect of increasing the magnitude of the experimental TCS, thereby alleviating, at least in part, this apparent paradox. Secondly, in the experiment the target was

a mixture of formic acid monomer and dimer while the calculation was for the monomer alone. This too could explain in part our current observation as to the magnitude discrepancy between our measurement and our most physical calculation. Having said that, in the electron channel Gianturco and Lucchese [7] found that the elastic cross sections for the dimer tended to be somewhat larger in magnitude than corresponding results for the monomer. If this were translated to the positron case, it would actually increase the observed disparity. However, this effect is yet to be quantified for positron scattering, and furthermore, as the dimer abundance is relatively small, we would anticipate it to be only a second-order effect in this case. Thirdly, the present calculation currently does not account for channels, e.g., vibrational excitation, electronic excitation, positronium formation, etc., which are open in the experiment. We would anticipate that if such channels could be included, in what would be a very difficult and computationally expensive calculation, the observed magnitude discrepancy might also be quantitatively rectified to some extent. Fourthly, we note that in the experiment, the formic acid sample exists in a distribution of allowed rotational states (j), given by the Boltzmann distribution, whereas the computation is for scattering from only $j=0$. This difference might therefore also explain some of the discrepancy observed in Fig. 3 between our measurements and calculations. Finally, it is well known [32] that the Born closure approach somewhat overestimates the lower-energy values of the elastic integral cross section, as the corresponding differential cross section diverges in the very forward angle direction. This limitation is not just restricted to the present work, it was also found earlier by Bouchiha *et al.* [32] in their elastic R-matrix electron-methanol results when they were compared to the experimental total cross-section data [33].

Although the electron-formic acid elastic collision cross section shows a shape resonance in the A'' symmetry [6,8,9,34], the cross section for positron collision is structureless and does not show such a resonance. This occurs because the short-range potential seen by the incoming positron is dominated by the repulsive nuclear potential. Therefore, the resulting potential (short range plus angular momentum barrier) cannot support a shape resonance.

V. CONCLUSIONS

We have reported results from a joint theoretical and experimental study into positron scattering from formic acid. Good qualitative (shape) agreement, particularly below the opening of the positronium formation channel, was found between them, with this comparison highlighting the important role played by both polarization and the permanent dipole moment of HCOOH in the scattering process. The experimental results also clearly indicated the importance of the opening of the positronium formation channel on the reaction.

ACKNOWLEDGMENTS

This work was supported under a Memorandum of Understanding between the University of Trento and the Flinders University node of the ARC Centre for Antimatter-Matter Studies. Financial support from DEST through its International Science Linkages (ISL) scheme, established under the Australian Government's innovation statement, "Building Australia's Ability," is gratefully acknowledged, as is Outside Studies Program assistance to M.J.B. from Flinders University. One of us (A.S.) thanks the International Centre for Theoretical Physics–TRIL Programme (Italy) for supporting his stay in Trento. M.H.F.B. and M.A.P.L. acknowledge support from the Brazilian agency Conselho Nacional de Desenvolvimento Científico e Tecnológico (CNPq). M.H.F.B. also acknowledges support from the Paraná state agency Fundação Araucária and from FINEP (under Project no. CT-Infra 1). M.A.P.L. acknowledges support from FAPESP. The authors also acknowledge computational support from Professor Carlos M. de Carvalho at DF-UFPR and from CENAPAD-SP. Finally, L.C. thanks the Provincia Autonoma di Bolzano (Italia) for financial support.

[1] B. Boudaiffa, P. Cloutier, D. Hunting, M. A. Huels, and L. Sanche, Science **287**, 1658 (2000).
[2] A. Pelc, A. Sailer, P. Scheier, M. Probst, N. J. Mason, E. Illenberger, and T. D. Märk, Chem. Phys. Lett. **361**, 277 (2002).
[3] V. S. Prabhudesai, D. Nandi, A. H. Kelkar, R. Parajuli, and E. Krishnakumar, Chem. Phys. Lett. **405**, 172 (2005).
[4] V. Vizcaino, M. Jelisavcic, J. P. Sullivan, and S. J. Buckman, New J. Phys. **8**, 85 (2006).
[5] K. L. Nixon, W. D. Lawrance, D. B. Jones, P. Euripides, S. Saha, F. Wang, and M. J. Brunger, Chem. Phys. Lett. **451**, 18 (2008).
[6] M. Allan, J. Phys. B **39**, 2939 (2006).
[7] F. A. Gianturco and R. R. Lucchese, Eur. Phys. J. D **39**, 399 (2006).
[8] C. S. Trevisan, A. E. Orel, and T. N. Rescigno, Phys. Rev. A **74**, 042716 (2006).
[9] M. H. F. Bettega, Phys. Rev. A **74**, 054701 (2006).
[10] A. Zecca, C. Perazolli, and M. J. Brunger, J. Phys. B **38**, 2079 (2005).
[11] A. Zecca, D. Sanyal, M. Chakrabarti, and M. J. Brunger, J. Phys. B **39**, 1597 (2006).
[12] A. Zecca, L. Chiari, A. Sarkar, and M. J. Brunger, J. Phys. B **41**, 085201 (2008).
[13] G. P. Karwasz, M. Barozzi, R. S. Brusa, and A. Zecca, Nucl. Instrum. Methods Phys. Res. B **192**, 157 (2002).
[14] K. R. Hoffman, M. S. Dababneh, Y.-F. Hsieh, W. E. Kauppila, V. Pol, J. H. Smart, and T. S. Stein, Phys. Rev. A **25**, 1393 (1982).
[15] A. S. Coolidge, J. Am. Chem. Soc. **50**, 2166 (1928).
[16] M. D. Taylor and J. Bruton, J. Am. Chem. Soc. **74**, 4151 (1952).
[17] H. J. Blaauw, F. J. de Heer, R. W. Wagenaar, and D. H.

Barends, J. Phys. B **10**, L299 (1977).
[18] A. Hamada and O. Sueoka, J. Phys. B **27**, 5055 (1994).
[19] A. Zecca and M. J. Brunger, in *Nanoscale Interactions and Their Applications: Essays in Honour of Ian Mc Carthy*, edited by F. Wang and M. J. Brunger (Research Signpost, Trivandrum, India, 2007), p. 21.
[20] T. Takaishi and Y. Sensui, Trans. Faraday Soc. **59**, 2503 (1963).
[21] G. Dalba, P. Fornasini, G. Ranieri, and A. Zecca, J. Phys. B **12**, 3787 (1979).
[22] J. S. E. Germano and M. A. P. Lima, Phys. Rev. A **47**, 3976 (1993).
[23] E. P. da Silva, J. S. E. Germano, and M. A. P. Lima, Phys. Rev. A **49**, R1527 (1994); Phys. Rev. Lett. **77**, 1028 (1996).
[24] E. P. da Silva, J. S. E. Germano, J. L. S. Lino, C. R. C. de Carvalho, A. P. P. Natalense, and M. A. P. Lima, Nucl. Instrum. Methods Phys. Res. B **143**, 140 (1998).
[25] *CRC Handbook of Chemistry and Physics*, edited by D. R. Lide, 79th ed. (CRC, Boca Raton, FL, 1998).
[26] C. W. Bauschlicher, J. Chem. Phys. **72**, 880 (1980).
[27] C. Winstead, V. McKoy, and M. H. F. Bettega, Phys. Rev. A **72**, 042721 (2005); M. H. F. Bettega, C. Winstead, and V. McKoy, *ibid.* **74**, 022711 (2006).
[28] M. A. Khakoo, J. Blumer, K. Keane, C. Campbell, H. Silva, M. C. A. Lopes, C. Winstead, V. McKoy, R. F. da Costa, L. G. Ferreira, M. A. P. Lima, and M. H. F. Bettega, Phys. Rev. A **77**, 042705 (2008).
[29] M. H. F. Bettega, R. F. da Costa, and M. A. P. Lima, Phys. Rev. A **77**, 052706 (2008).
[30] P. Chaudhuri, M. T. do N. Varella, C. R. C. de Carvalho, and M. A. P. Lima, Phys. Rev. A **69**, 042703 (2004).
[31] C. M. Surko, G. F. Gribakin, and S. J. Buckman, J. Phys. B **38**, R57 (2005).
[32] D. Bouchiha, J. D. Gorfinkiel, L. G. Caron, and L. Sanche, J. Phys. B **40**, 1259 (2007).
[33] C. Szmytkowski and A. M. Krzysztofowicz, J. Phys. B **28**, 4291 (1995).
[34] T. N. Rescigno, C. S. Trevisan, and A. E. Orel, Phys. Rev. Lett. **96**, 213201 (2006).